J Solid State Electrochem (2016) 20:3367–3373
DOI 10.1007/s10008-016-3305-5

ORIGINAL PAPER

Kinetics of Na|CF_x and Li|CF_x systems

Andrzej Lewandowski[1] · **Paweł Jakobczyk**[1]

Received: 29 January 2016 / Revised: 20 June 2016 / Accepted: 22 June 2016 / Published online: 30 June 2016

Abstract Properties of CF_x/Li and CF_x/Na cells were examined while using galvanostatic charging/discharging, electrochemical impedance spectroscopy and scanning electron microscopy (SEM). The capacity during the first cycle was as high as ca. 1000 mAh g^{-1}. Such an electrode is suitable for primary CF_x/Li and CF_x/Na batteries. SEM images of CF_x cathode showed that during discharging it was transformed into amorphous carbon and LiF or NaF crystals (of diameter of ca. 5–20 μm). These systems (C + LiF or C + NaF) cannot be reversibly converted back into CF_x/Li or CF_x/Na, respectively. Exchange current densities are between 10^{-7} Acm^{-2} and 10^{-9} Acm^{-2} when working with $LiPF_6$ and $NaPF_6$ electrolytes (1.12×10^{-7} Acm^{-2} and 6.82×10^{-9} Acm^{-2}, respectively). Those values are low and indicate that the charge transfer process may be the rate-determining step. Activation energies for the charge transfer process were 57 and 72 kJ mol^{-1} for CF_x/$LiPF_6$ and CF_x/$NaPF_6$ systems, respectively. Higher activation energy barrier for the $CF/Na^+ + e^- \rightarrow C + NaF$ reaction results in lower observed exchange current density in comparison to the system with lithium ions.

Introduction

In Li-ion batteries, lithium metal anode is replaced by lithium-intercalated carbons (LiC_x) due to the irreversible behavior of this metal. Hence, battery contains lithium in the form of intercalated compounds and electrolyte. Total amount of lithium in seawater is high (2.4×10^{11} tons) but the concentration is constant and low: 2.5×10^{-5} mol l^{-1} (0.173 mg l^{-1}) in contrast to sodium (0.468 mol l^{-1} or 10.77 g l^{-1}) [1]. Therefore, lithium resources are brine (Argentina, Chile, and the USA) and minerals whereas sodium can be electrochemically recovered from abounded sodium chloride. In addition, lake brine can contain more magnesium than lithium (for example in the ratio of 40:1) [2]. As a result, sodium is cheaper in comparison to lithium—US$5000 and US$150 for 1 ton of Li_2CO_3 and Na_2CO_3, respectively [3]. While carbon lithium-intercalated anodes work reversibly for ca. 10^3 cycles [4–10] the carbon-sodium system does not show such a promising reversible capacity [11–16]. Therefore, Li-ion systems are fully commercialized but Na-ion batteries are still under research [3, 12, 17–37]. On the other hand, there is a demand for primary power sources of high energy density. Both metallic lithium and sodium are sufficient anode materials for such batteries due to their capacity (Li: 3829 mAh g^{-1} and Na: 1165 mAh g^{-1}) [3]. Due to much lower sodium price (in comparison to lithium), it seems to be a more attractive candidate for metallic anode. Another problem is a selection of a suitable cathode of the capacity comparable to that characteristic of Li or Na anodes. Many cathodic systems were selected, but their capacity was usually of the order of 100 mAh g^{-1} [11]. Fluorinated graphite, CF_x, was synthesized in 1934 and it was shown that it can be used as a cathode and even Li/CF_x battery was commercialized [38]. Then different fluorinated CF_x materials of different fluorination level were prepared [39, 40]. Discharge capacities of different CF_x materials are reported to be between 600 and 900 mAh g^{-1} [40, 41] with open circuit potential against metallic lithium between 2.4 and 3.5 V, depending on CF_x material and electrolyte [39, 42] and energy density of 2000 Wh kg^{-1} [43]. The theoretical capacity of CF_x is 865 mAh g^{-1} for $x = 1$ and decreases as the x value increases [43]. It was demonstrated that CF_x

✉ Andrzej Lewandowski
andrzej.lewandowski@put.poznan.pl

[1] Faculty of Chemical Technology, Poznan University of Technology, PL-60 965 Poznan, Poland

materials of high fluorination level did not show enhanced capacity, as CF_2 groups were electrochemically inactive [40]. While Li/CF_x battery was extensively studied [44–54], to our knowledge the electrochemical properties of Na/CF_x system were reported once in 2014 [55]. The papers were focused on systems capacity and mechanism of electrochemical and chemical processes. Nonetheless, power of electrochemical systems depends on kinetic limits. The general aim of the present study has been kinetic characterization of Na/CF_x system and its comparison to Li/CF_x battery.

Experimental

Materials

Sodium sticks (Aldrich), lithium foil (0.75 mm thick, Aldrich), vinylene carbonate (VC, Aldrich), ethylene carbonate (EC, Aldrich), propylene carbonate (PC, Aldrich), dimethyl carbonate (DMC, Aldrich) lithium hexafluorophosphate ($LiPF_6$, Aldrich), sodium hexafluorophosphate ($NaPF_6$, Aldrich), graphite fluoride (CF_x, ACS Material), carbon black (CB, Alfa Aesar), poly(vinylidene fluoride) (PVdF, Fluka), and *N*-methyl-2-pyrrolidinone (NMP, Fluka) were used as received from suppliers.

Vinylene carbonate was stored at a max temperature of 8 °C to prevent its from spontaneous polymerization. Liquid electrolytes (90 wt% of 1 M $LiPF_6$ or 1 M $NaPF_6$ in PC-DMC (1:1 wt) + 10 wt% of VC) were obtained by dissolution of solid $LiPF_6$ or $NaPF_6$ salt in liquid mixture PC-DMC (90 wt%) + VC (10 wt%). Solutions of electrolytes were prepared and cells were assembled in a glove box in the dry argon atmosphere.

CF_x electrode was prepared with a composition of 80 wt% CF_x, 10 wt% carbon black (CB) conductive additive and 10 wt% polyvinylidene fluoride (PVDF) binder by mixing calculated amounts of CF_x, CB and PVDF with 1-methyl-2pyrrolidone (NMP) solvent. The suspension of solid components in NMP was cast on Au current collector. After solvent (NMP) evaporation at 120 °C in a vacuum, a layer of the carbon electrode was formed containing the active material (CF_x), electronic conductor (CB), and the binder (PVdF). The electrode contained typically 3–6 mg of the fluoride graphite. A round-shaped metallic sodium or lithium counter electrode were formed from stick metallic sodium and cut-off from the metallic lithium foil, respectively. The surface area of the Li and Na electrodes was 1.27 cm^2.

Measurements

The CF_x (CF_x + CB + PVdF) electrodes were separated from sodium or lithium by glass microfiber separator (GF/A, Whatman) soaked with the electrolyte. CF_x|electrolyte|sodium and CF_x|electrolyte|lithium systems were placed in an adapted 0.5″ Swagelok® connecting tube. Electrochemical properties of cells were characterized using electrochemical impedance spectroscopy (EIS) and galvanostatic charging/discharging tests. Galvanostatic curves of charging/discharging and impedance spectra (frequency range of 100 kHz–10 mHz, at open circuit potential and amplitude of 10 mV) were obtained using a frequency response analyzer (multichannel Interface 1000, Potentiostat/Galvanostat system, Gamry, USA). Deconvolution of spectra was performed with the Gamry software. The morphology of graphite fluoride electrodes (pristine and after intercalation of sodium and lithium) were analyzed using electron scanning microscope (TESCAN Vega 5153, Czech Republic). BET surface of pristine CF_x material was determined with Autosorb iQ apparatus (Quantochrome Instruments, UK).

Results and discussion

Galvanostatic charging/discharging

CF_x cathode was tested galvanostatically in CF_x |1 M $LiPF_6$ PC-DMC 10 % VC|Li and CF_x|1 M $NaPF_6$ PC-DMC 10 % VC|Na systems. As a matter of fact, in all experiments the mass of the lithium or sodium anodes was much higher (ca. 40 mg) or electrochemically equivalent to the mass of the cathode. Open circuit potential of the cells measured immediately after their assembling was ca. 3.3 V. Figure 1 shows the discharging/charging curves for both systems with current densities of 50–5 mA g^{-1}. Voltage versus product of time *t* and current *I* (usually assumed to reflect the electrode capacity *q*) in both cases showed two distinct plateaus. In the case of CF_x|Li cell the first plateau occurs at voltages of 2.34–2.1 V and the second 1.6–1.36 V, while CF_x|Na system at ca. 2.0 V (1.99–1.79 V) and 1.3–1.05 V. Cells containing electrolytes without VC showed the second plateau at lower voltage of ca. 0.5 V. This is why the experiments were performed using electrolytes containing VC as an additive. Voltage versus *q* curves for the systems under study were published previously for voltages not lower than ca. 2 V and the cathode material was obtained from different source [55]. This makes both systems difficult to compare. However, the initial capacity of the first plateau of the Na/CF_x was reported to be ca. 1000 mAh g^{-1} [55], to decrease to ca. 786 and 409 mAh g^{-1} after the second and sixth cycle, respectively (at a current density of 200 mAh g^{-1}, discharge to 1.5 V). This suggests rather irreversible nature of the system. It was stated that "obviously, Na/CF_x batteries should be further improved [55]." Tested cells in this work showed two distinct plateaus within the $q = I.t$ value of ca. 1000 mAh g^{-1}, including the second plateau with *q* at a lower level ca. three times, but energy delivered is even lower as the potential of the second plateau

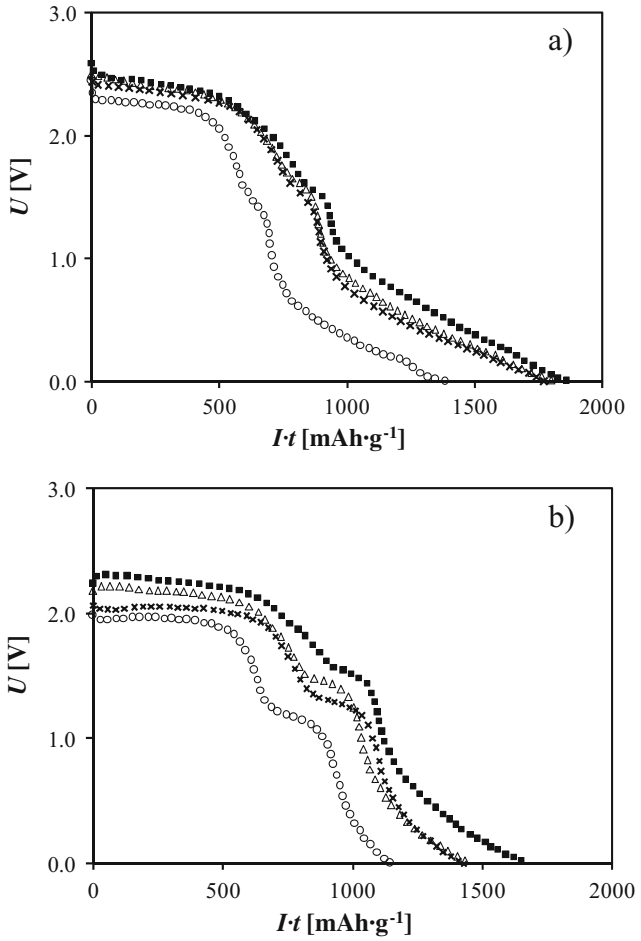

Fig. 1 Discharging curves (50 mA: *white circle*, 25 mA: *multiplication sign*, 10 mA: *white triangles* and 5 mA: *black square*) for **a** CF_x/Li and **b** CF_x/Na systems. Electrolyte: 1 M $LiPF_6$ in PC + DMC (1:1) + 10 wt % VC

is ca. 1 V (and not 2 V). Poor reversibility and capacity fading during cycling within the first plateau indicate that CF_x|Na systems are rather good candidates for primary batteries and not rechargeable ones. Free enthalpy associated with CF_x|Na^+ cathode discharging till the end of the first plateau was ca. 2 V × 600 mAh $g^{-1} \approx 4.32$ kJ g^{-1} while the corresponding value for the second plateau is only ca. 1.3 V × 211 mAh $g^{-1} = 0.99$ kJ g^{-1}. Integration of $I = f(t)$ curves shown in Fig. 1 gave higher overall capacity (ca. 1000 mAh g^{-1}) higher amount of energy delivered to be 6.06 and 5.79 kJ g^{-1} for CF_x|Li and CF_x|Na primary batteries (expressed versus CF_x mass), respectively. At lower current regimes capacitance calculated as $q = It$ is somewhat higher (ca. 7 %). Discharge curves and CF_x capacities for CF_x|Na system working with 1 M $LiPF_6$ in EC + DMC (1:1) + 10 wt% VC were similar to those obtained for the electrolyte containing PC instead of EC. Potential recorded during Li/CF_x or Na/CF_x discharging is a mixed potential of electrodefluorination of CF_x material to carbon and F^- anions (the first plateau) and electrolyte decomposition [56]. After electrochemical de-fluorination, the surface inactive CF_2 groups are eliminated to form a more electronic and ionic conductive surface [57]. Figure 2 shows SEM images of pristine CF_x electrode (Fig. 2a) and then after its discharging (Fig. 2b: CF_x|Li and Fig. 2c: CF_x|Na). It can be seen that the pristine CF_x material consists of fluorinated graphite particles, which were transformed during the electrode reaction into amorphous carbon and LiF or NaF crystals of diameter of ca. 5–20 μm.

Impedance studies

Figure 3 shows electrochemical impedance spectra (EIS) of CF_x electrode taken after CF_x|Li and CF_x|Na systems assembling (Fig. 3a, b). Spectra consist of two parts: a semicircle and a straight line at lower frequencies. Corresponding spectra for discharged systems are shown in Fig. 3c, d. It can be seen that impedance decreased considerably. This is probably due to conversion of CF_x into solid C/LiF or C/NaF. In addition, lithium and sodium anodes without CF_x counter electrode do not show such high impedances (Fig. 3e, f). This suggests that

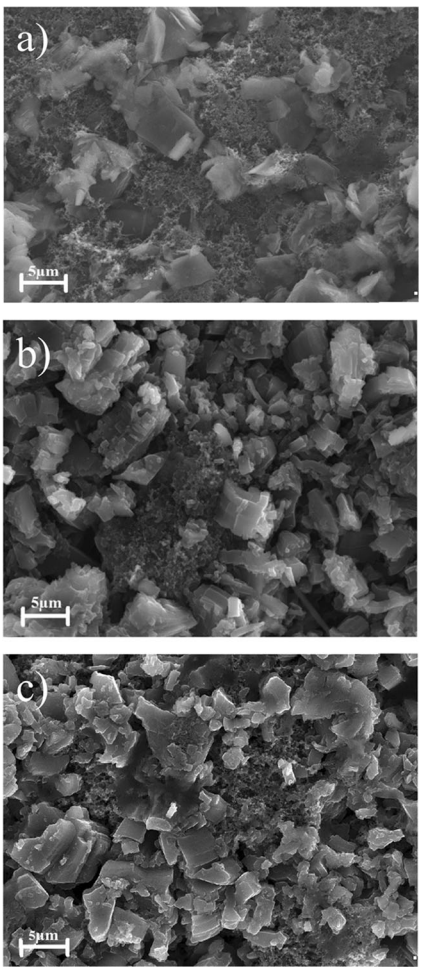

Fig. 2 SEM images of CF_x cathode **a** pristine and after discharging **b** in CF_x/Li and **c** in CF_x/Na systems

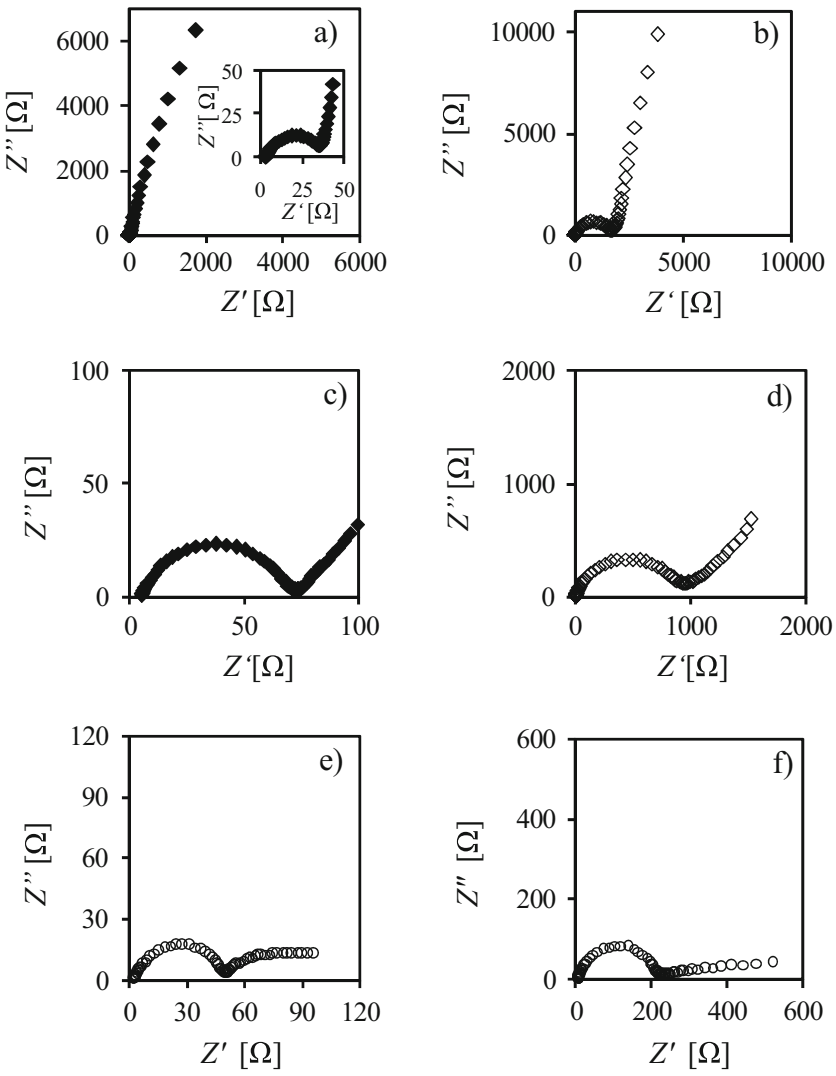

Fig. 3 Impedance spectra of CF_x/Li and CF_x/Na systems before (**a**, **b**) and after their discharging, (**c**, **d**) as well as Li/Li (**e**) and Na/Na (**f**) symmetric cells

CF_x material is responsible for the high total impedance of CF_x/Li and CF_x/Na systems. Goodness of the fit was close to 10^{-4}–10^{-5} (Fig. 4 shows examples of the fits overlaid with the experimental data). On the other hand, total impedance of both systems decreased considerably with temperature increase (Fig. 5). Curves shown in Fig. 5 were deconvoluted taking into account two time constants *RC*, due to the SEI layer (R_{SEI}, C_{SEI}) and the charge transfer process which occurs at the double layer formed between SEI and the anode (R_{ct}, C_{dl}). The straight line at the low frequency section is due to the Li^+ and Li diffusion. Therefore, the equivalent circuit consisted of electrolyte resistance (R_{el}) in series with two time constants (R and C in parallel: R_{SEI}, C_{SEI} and R_{ct}, C_{ct}) and Warburg element Z_W.

The value of the charge transfer resistance at 25 °C estimated from the deconvolution procedure was 57 Ω for CF_x/Li and as high as 862 Ω for CF_x/Na. Determined R_{ct} resistances can be expressed versus real surface area of cathode material $S_{BET} = 93.6\ m^2\ g^{-1}$, estimated from BET measurement. The mass of CF_x cathode material used in impedance experiments was 4.32 and 4.72 mg in CF_x/Li and CF_x/Na cells, respectively. This leads to electrodes real surface area *A* and corresponding $R_{ct}.A$ values expressed in Ω cm^2 (Table 1). Charge transfer resistances may be converted into exchange current densities j_o (1):

$$j_0 = \frac{RT}{F}\frac{1}{SR_{ct}} \tag{1}$$

Exchange current densities listed in Table 1 are of the order of 10^{-7} Acm^{-2} when working with $LiPF_6$ (1.12×10^{-7} Acm^{-2}) and ca. two orders of magnitude lower for $NaPF_6$ electrolyte (6.82×10^{-9} Acm^{-2}). Those values are low and indicate that the charge transfer process may be the rate-determining step. In addition, the CF_x material is resistive; however, even during a short time of discharge, it is coated with conductive carbon particles [58, 59]. It has been shown for the Li/CF_x system that at low rates of discharge (through a fixed resistive load

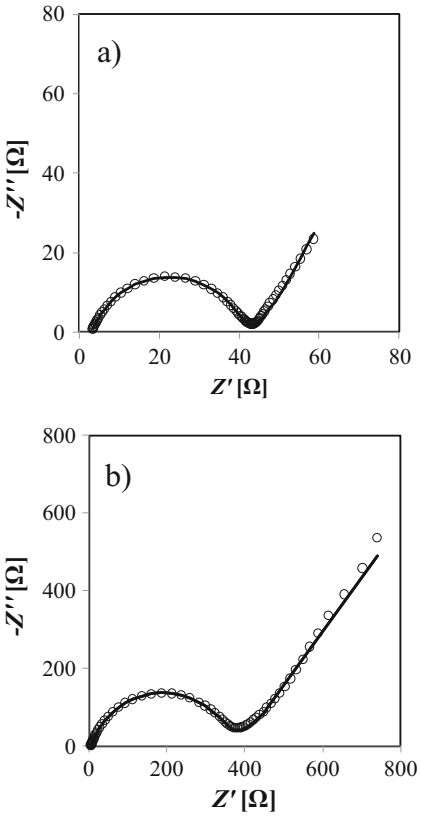

Fig. 4 Impedance plots of **a** $LiPF_6/CF_x$ (goodness of fit: 1.93×10^{-4}) and **b** $NaPF_6/CF_x$ (goodness of fit: 3.77×10^{-4}). Counter and reference electrode: metallic lithium or sodium. $T = 35$ °C

Table 1 Mass m and real surface area S of CF_x cathodes used in impedance experiments together with kinetic parameters for cathodic reaction: charge transfer resistance R_{ct}, product SR_{ct} and corresponding exchange current density j_o

Anode	Electrolyte	m/mg	S/cm^2	R_{ct}/Ω	SR_{ct}/Ωcm^2	j_o/Acm^{-2}
Li	$LiPF_6$	4.32	4.04×10^3	57	2.30×10^5	1.12×10^{-7}
Na	$NaPF_6$	4.72	4.42×10^3	862	3.81×10^6	6.82×10^{-9}

attached to each tested cell) the system obeys Tafel kinetics and transport properties are of negligible importance [58, 59]. Consequently, this observation suggested that the kinetic rate constant was very small [58].

The resistance R_{ct}, obtained at different temperatures, gave $\ln R^{-1} = f(T^{-1})$ straight line with a slope indicating activation energy $E^{\#}$ of the overall process in the cell during its discharging. Obtained activation energies for the charge transfer process were 57 and 72 kJ mol^{-1} for $CF_x/LiPF_6$ and $CF_x/NaPF_6$ systems, respectively. Higher activation energy barrier for the $CF/Na^+ + e^- \rightarrow C + NaF$ reaction results in lower observed exchange current density in comparison to the system with lithium ions.

Deconvolution of impedance spectra of Li/Li and Na/Na systems, without CF_x cathode (shown in Fig. 3e, f) gave charge transfer resistance values for the Li/Li^+ (48 Ω) and (201 Ω). Taking into account anodes surface area of

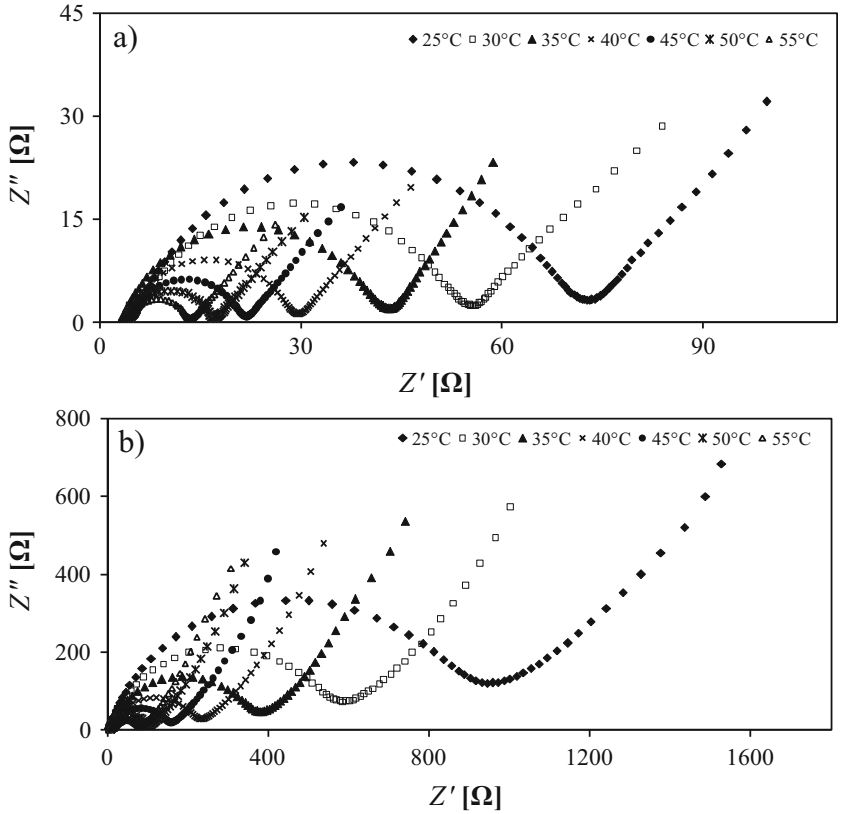

Fig. 5 Impedance spectra of **a** CF_x/LiF and **b** CF_x/NaF systems, (after discharging to 0.35 V). Counter and reference electrode: metallic lithium or sodium

1.27 cm^2, resulting exchange current densities are 0.41 and 0.10 mA cm^{-2} for Li/Li^+ and Na/Na^+, respectively. Charge transfer process for sodium is slower in comparison to that characteristic of lithium; however, 3–4 orders of magnitude faster in comparison to that characteristic of CF_x cathode. Kinetics of Li/Li^+ and Na/Na^+ was also investigated in ionic liquids [60–65]. In the literature, the charge transfer reaction is described by exchange current density, j_o, rate constant k_o or corresponding resistance R_{ct}, which are mutually related. Cyclic voltammetry experiments on Pt and Ni electrodes gave similar value of charge transfer rate constant $k_o \sim 10^{-5}$ cm s^{-1} for both Li/Li^+ [60, 62] and Na/Na^+ [61] systems. In the case of metallic lithium and sodium electrodes a protective layer of the solid electrolyte interphase (SEI) is formed. In such a case, the charge transfer reaction takes place at the interphase between two solids: Li/SEI or Na/SEI. This makes recalculation of k_o into R_{ct} or j_o difficult.

Conclusions

Cyclability of the CF_x cathode is generally poor. However, the capacity at the first cycle is as high as ca. 1000 mAh g^{-1}. Such an electrode is suitable for primary CF_x/Li and CF_x/Na batteries. During discharging, the CF_x cathode was transformed into amorphous carbon and LiF or NaF crystals of diameter of ca. 5–20 μm. These systems (C + LiF or C + NaF) cannot be reversibly converted back into CF_x/Li or CF_x/Na, respectively. Exchange current densities are of the order of 10^{-7} Acm^{-2}–10^{-9} Acm^{-2} when working with $LiPF_6$ and $NaPF_6$ electrolytes (1.12×10^{-7} Acm^{-2} and 6.82×10^{-9} Acm^{-2}, respectively). Those values are low and indicate that the charge transfer process may be the rate-determining step. Activation energies for the charge transfer process were 57 kJ mol^{-1} and 72 kJ mol^{-1} for $CF_x/LiPF_6$ and $CF_x/NaPF_6$ systems, respectively. Higher activation energy barrier for the $CF/Na^+ + e^- \rightarrow C + NaF$ reaction results in lower observed exchange current density in comparison to the system with lithium ions.

Acknowledgments Support of the grant NCN UMO/2013/09/B/ST4/00107 is gratefully acknowledged.

References

1. Schwochau K (1984) Extraction of metals from sea water. Top Curr Chem 124:91–133
2. Liu X, Chen X, He L, Zhao Z (2015) Study on extraction of lithium from salt lake brine by membrane electrolysis. Desalination 376: 35–40
3. Slater MD, Kim D, Lee E, Johnson CS (2013) Sodium-Ion Batteries. Adv Funct Mater 23:947–958
4. Scrosati B, Garche J (2010) Lithium batteries: status, prospects and future. J Power Sources 195:2419–2430
5. Goriparti S, Miele E, De Angelis F, Di Fabrizio E, Proietti Zaccaria E, Capiglia C (2014) Review on recent progress of nanostructured anode materials for Li-ion batteries. J Power Sources 257:421–443
6. Xu K (2014) Electrolytes and interphases in Li-ion batteries and beyond. Chem Rev 114:11503–11618
7. Nitta N, Wu F, Lee JT, Yushin G (2014) Li-ion battery materials: present and future. Mater Today 18:252–264
8. Roy P, Srivastava SK (2015) Nanostructured anode materials for lithium ion batteries. J Mater Chem A 3:2454–2484
9. Diouf B, Pode R (2015) Potential of lithium-ion batteries in renewable energy. Renew Energy 76:375–380
10. Marom R, Amalraj SF, Leifer N, Jacob D, Aurbach D (2011) A review of advanced and practical lithium battery materials. J Mater Chem 21:9938–9954
11. Xiang X, Zhang K, Chen J (2015) Recent advances and prospects of cathode materials for sodium-ion batteries. Adv Mater 27:5343–5364
12. Go D-Y, Park J, Noh P-J, Cho G-B, Ryu H-S, Nam T-H et al (2014) Electrochemical properties of monolithic nickel sulfide electrodes for use in sodium batteries. Mater Res Bull 58:190–194
13. Park J, Kim J-S, Park J-W, Nam T-H, Kim K-W, Ahn J-H et al (2013) Discharge mechanism of MoS_2 for sodium ion battery: electrochemical measurements and characterization. Electrochim Acta 92:427–432
14. Ryu H, Kim T, Kim K, Ahn JH, Nam T, Wang G et al (2011) Discharge reaction mechanism of room-temperature sodium-sulfur battery with tetraethylene glycol dimethyl ether liquid electrolyte. J Power Sources 196:5186–5190
15. Wongittharom N, Wang C, Wang Y, Yang C, Chang J (2014) Ionic liquid electrolytes with various sodium solutes for rechargeable Na/$NaFePO_4$ batteries operated at elevated temperatures. ACS Appl Mater Interfaces 6:17564–17570
16. Wang L, Lu Y, Liu J, Xu M, Cheng J, Zhang D (2013) A superior low-cost cathode for a Na-ion battery. Angew Chemie-Int Ed 52: 1964–1967
17. Xie X, Ao Z, Su D, Zhang J, Wang G (2015) MoS_2/graphene composite anodes with enhanced performance for sodium-ion batteries: the role of the two-dimensional heterointerface. Adv Funct Mater 25:1393–1403
18. Deng W, Liang X, Wu X, Qian J, Cao Y, Ai X et al (2013) A low cost, all-organic Na-ion battery based on polymeric cathode and anode. Sci Rep 3:1–6
19. Billaud J, Cle J, Armstrong AR, Rozier P, Grey CP, Bruce PG (2014) β-$NaMnO_2$: a high-performance cathode for sodium-ion batteries. J Am Chem Soc 136:17243–17248
20. Kumar PR, Jung YH, Kim DK (2015) High performance of MoS_2 microflowers with a water-based binder as an anode for Na-ion batteries. RSC Adv 5:79845–79851
21. Yang YY, Yang X, Zhang Y, Hou H, Jing M, Zhu Y et al (2015) Cathodically induced antimony for rechargeable Li-ion and Na-ion batteries: the influences of hexagonal and amorphous phase. J Power Sources 282:358–367
22. Yuan D, He W, Pei F, Wu F, Wu Y, Qian J et al (2013) Synthesis and electrochemical behaviors of layered $Na_{0.67}[Mn_{0.65}Co_{0.2}Ni_{0.15}]O_2$ microflakes as a stable cathode material for sodium-ion batteries. J Mater Chem A 1:3895–3899
23. Shen Y, Wang X, Hu H, Jiang M, Yang X, Shu H (2015) A graphene loading heterogeneous hydrated forms iron based fluoride

nanocomposite as novel and high-capacity cathode material for lithium/sodium ion batteries. J Power Sources 283:204–210
24. Barpanda P, Lu J, Ye T, Kajiyama M, Chung S-C, Yabuuchi N et al (2013) A layer-structured $Na_2CoP_2O_7$ pyrophosphate cathode for sodium-ion batteries. RSC Adv 3:3857–3860
25. Lu Y, Wang L, Cheng J, Goodenough JB (2012) Prussian blue: a new framework of electrode materials for sodium batteries. Chem Commun 48:6544–6546
26. Kang YH, Liu Y, Cao K, Zhao Y, Jiao L, Wang Y et al (2015) Update on anode materials for Na-ion batteries. J Mater Chem A 3:17899–17913
27. Kundu D, Tripathi R, Popov G, Makahnouk WRM, Nazar LF (2015) Synthesis, structure and Na-ion migration in $Na_4NiP_2O_7F_2$: a prospective high voltage positive electrode material for the Na-ion battery. Chem Mater 27:885–891
28. Han MH, Gonzalo E, Singh G, Rojo T (2015) A comprehensive review of sodium layered oxides: powerful cathodes for Na-ion batteries. Energy Environ Sci 8:81–102
29. Kim Y, Ha K-H, Oh SM, Lee KT (2014) High-capacity anode materials for sodium-ion batteries. Chem-A Eur J 20:11980–11992
30. Yabuuchi N, Kubota K, Dahbi M, Komaba S (2014) Research development on sodium-ion batteries. Chem Rev 114:11636–11682
31. Palomares V, Casas-Cabanas M, Castillo-Martínez E, Han MH, Rojo T (2013) Update on Na-based battery materials. A growing research path. Energy Environ Sci 6:2312–2337
32. Hong SY, Kim Y, Park Y, Choi A, Choi N-S, Lee KT (2013) Charge carriers in rechargeable batteries: Na ions vs. Li ions. Energy Environ Sci 6:2067–2081
33. Bommier C, Ji X (2015) Recent development on anodes for Na-ion batteries. Isr J Chem 55:486–507
34. Ellis BL, Nazar LF (2012) Sodium and sodium-ion energy storage batteries. Curr Opin Solid State Mater Sci 16:168–177
35. Pan H, Hu Y-S, Chen L (2013) Room-temperature stationary sodium-ion batteries for large-scale electric energy storage. Energy Environ Sci 6:2338–2360
36. Palomares V, Serras P, Villaluenga I, Hueso KB, Carretero-González J, Rojo T (2012) Na-ion batteries, recent advances and present challenges to become low cost energy storage systems. Energy Environ Sci 5:5884–5901
37. Dahbi M, Yabuuchi N, Kubota K, Tokiwa K, Komaba S (2014) Negative electrodes for Na-ion batteries. Phys Chem Chem Phys 16:15007–15028
38. Nakajama T (1999) Carbon-fluorine compounds as battery materials. J Fluorine Chem 100:57–61
39. Guerin K, Dubois M, Hamwi A (2006) Electrochemical discharge mechanism of fluorinated graphite used as electrode in primary lithium batteries. J Phys Chem Solids 67:1173–1177
40. Giraudet J, Delabarre C, Guerin K, Dubois M, Masin F, Hamwi A (2006) Comparative performances for primary lithium batteries of some covalent and semi-covalent graphite fluorides. J Power Sources 158:1365–1372
41. Delabarre C, Dubois M, Giraudet J, Guerin K, Hamwi A (2006) Electrochemical performance of low temperature fluorinated graphites used as cathode in primary lithium batteries. Carbon 44:2543–2548
42. Zhang Q, D'Astorg S, Xiao P, Zhang X, Lu L (2010) Carbon-coated fluorinated graphite for high energy and high power densities primary lithium batteries. J Power Sources 195:2914–2917
43. Zhang Q, Takeuchi KJ, Takeuchi ES, Marschilok AC (2015) Progress towards high-power Li/CFx batteries: electrode architectures using carbon nanotubes with CFx. Chem Phys 17:22504–22518
44. Hamwi A, Guérin K, Dubois M (2005) Fluorine-intercalated graphite for lithium batteries. In: Nakajima T, Groult H (eds) Fluorinated materials for energy conversion. Elsevier Ltd, Oxford, pp 369–395
45. Whitacre J, Yazami R, Hamwi A, Smart MC, Bennett W, Prakash GKS, Miller T, Bugga R (2006) Low operational temperature Li–CF_x batteries using cathodes containing sub-fluorinated graphitic materials. J Power Sources 160:577–584
46. Ahmad Y, Dubois M, Guérin K, Hamwi A, Zhang W (2015) Pushing the theoretical limit of Li–CF_x batteries using fluorinated nanostructured carbon nanodiscs. Carbon 94:1061–1070
47. Guérin K, Yazami R, Hamwi A (2014) Hybrid-type graphite fluoride as cathode material in primary lithium batteries. Electrochem Solid St 7:A159–A162
48. Delabarre C, Dubois M, Giraudet J, Guerin K, Yazami R, Hamwi A (2007) Comparative electrochemical study of low temperature fluorinated graphites used as cathode in primary lithium batteries. T Electrochem Soc 3:153–163
49. Dubois M, Guérina K, Zhanga W, Ahmada Y, Hamwi A, Fawal Z, Kharbache H, Masin F (2012) Tuning the discharge potential of fluorinated carbon used as electrode in primary lithium battery. Electrochim Acta 59:485–491
50. Amatucci GG, Pereira N (2007) Fluoride based electrode materials for advanced energy storage devices. J Fluorine Chem 128:243–262
51. Read J, Collins E, Piekarski B, Zhang S (2011) LiF formation and cathode swelling in the Li/CF_x battery. J Electrochem Soc 158: A504–A510
52. Zhang SS, Foster D, Wolfenstine J, Read J (2009) Electrochemical characteristic and discharge mechanism of a primary Li/CF_x cell. J Power Sources 187:233–237
53. Lam P, Yazami R (2006) Physical characteristics and rate performance of $(CF_x)_n$ ($0.33 < x < 0.66$) in lithium batteries. J Power Sources 153:354–359
54. Yazami R, Hamwi A, Guérin K, Ozawa Y, Dubois M, Giraudet J, Masin F (2007) Fluorinated carbon nanofibres for high energy and high power densities primary lithium batteries. Electrochem Commun 9:1850–1855
55. Liu W, Li H, Xie J-Y, Fu Z-W (2014) Rechargeable room-temperature CF_x-sodium battery. ACS Appl Mater Interface 6: 2209–2112
56. Hunger HF, Ellison JE (1975) Rate capability and electrochemical stability of carbon fluoride compounds in organic electrolytes. J Electrochem Soc 122:1288–1291
57. Dai Y, Cai S, Wu L, Yang W, Xie J, Wen J, Zheng J-C, Zhu Y (2014) Surface modified cathode material for ultrafast discharge and high energy density. J Mater Chem A 2:20896–20901
58. Davis S, Takeuchi ES, Tiedemann W, Newman J (2007) Simulation of the Li-CF_x system. J Electrochem Soc 154:A477–A480
59. Davis S, Takeuchi ES, Tiedemann W, Newman J (2008) Simulation of pulse discharge of the Li-CF_x system. J Electrochem Soc 155: A24–A28
60. Wibowo R, Ward Jones SE, Compton R (2009) Kinetic and thermodynamic parameters of the Li/Li + couple in the room temperature ionic liquid N-butyl-N-metylpyrrolidinium bis(trifluoromethylsulfonyl) imide in the temperature range 298–318 K: a theoretical and experimental study using Pt and Ni electrodes. J Phys Chem B113:12293–12298
61. Wibowo R, Aldous L, Rogers EI, Ward Jones SE, Compton RG (2010) A study the Na/Na^+ redox couple in some room temperature ionic liquids. J Phys Chem C114:3618–3626
62. Wibowo R, Ward Jones SE, Compton RG (2010) Investigating the electrode kinetics of the Li/Li^+ couple in a wide range of room temperature ionic liquids at 298 K. J Chem Eng Data 55:1374–1376
63. Lewandowski A, Swiderska-Mocek A, Waliszewski L, Galinski M (2012) Lithium redox behaviour in N-methyl-N-propylpyrrolidinium bis(trifluoromethanesulfonyl) imide room temperature ionic liquid. J Power Sources 197:292–296
64. Lewandowski A, Biegun M, Galinski M (2012) Kinetics of Li^+ reduction in 1-methyl-3-propylpiperidinium bis(trifluoromethylsulfonyl) imide room temperature ionic liquid. Electrochim Acta 63:204–208
65. Lewandowski A, Biegun M, Galinski M, Swiderska-Mocek A (2013) Kinetic analysis of Li/Li^+ interphase in an ionic liquid electrolyte. J Appl Electrochem 43:367–374